# The dependence of osteoblastic response on variations in the chemical composition and physical properties of hydroxyapatite

S. BEST*, B. SIM[‡§], M. KAYSER[‡], S. DOWNES[‡§]
** IRC in Biomedical Materials, Queen Mary and Westfield College, Mile End Road, London, E1 4NS, England*
*[‡] IRC in Biomedical Materials, Institute of Orthopaedics, University College and Middlesex Schools of Medicine, Brockley Hill, Stanmore, Middlesex, HA7 4LP, England*

Two synthetic hydroxyapatite powders (A and B), supplied by different manufacturers, were physically and chemically characterized before being die pressed and sintered at 1250 °C. The powders were characterized using X-ray diffraction (XRD), infrared spectroscopy (IRS), X-ray fluorescence, surface area analysis (BET), particle size analysis and scanning electron microscopy (SEM). The materials were then pressed and sintered to produce hydroxyapatite discs of similar densities and grain sizes for *in vitro* evaluation. The ceramics were seeded with osteoblastic cells and after 15 days in culture the cell morphology was assessed using scanning electron microscopy (SEM), the ultrastructure of the cells was studied using transmission electron microscopy (TEM) with EDAX, and the rate of cell growth was assessed using biochemical techniques. The results clearly showed that the rate of cell proliferation but not the rate of alkaline phosphatase production, was highly dependent on the composition of the hydroxyapatite powders that were used to make the ceramic discs. The ultrastructural studies confirmed the relative viabilities of the cells and the nature of the ceramic interface indicating visually the marked differences in the performance of the two materials.

## 1. Introduction

Hydroxyapatite has been investigated as a bone replacement material for approximately 25 years [1–16] and has also been extensively studied using cell culture techniques [17–20] and also *in vivo* [21–26]. The profound effect of hydroxyapatite powder morphology on the sintering behaviour of the material has been reported previously [12, 15]. However, despite its importance in the bioceramics field there remains a need to correlate the chemical and physical composition of hydroxyapatite with cellular interactions.

This paper documents preliminary results in trials with two hydroxyapatite powders from different sources. The synthetic hydroxyapatite powders were chemically and physically characterized and then the powders were pressed and sintered to produce ceramic discs of similar densities and grain sizes for *in vitro* evaluation. The ceramics were seeded with human osteoblast-like cells. The cell morphology was assessed using scanning electron microscopy (SEM), the ultrastructure of the cells was studied using transmission electron microscopy (TEM) with EDAX and the rate of cell growth was assessed using biochemical techniques. The work reported in this paper forms part of a larger programme to study the *in vitro* response of human osteoblast-like cells to ceramics of contrasting microstructure and composition.

## 2. Methods

### 2.1. Powder characterization

Two synthetic hydroxyapatite powders (powders A and B) were chemically and physically characterized using X-ray diffraction (XRD), infrared spectroscopy (IRS), X-ray fluorescence, surface area analysis (BET), particle size analysis and scanning electron microscopy (SEM). X-ray diffraction was performed on powder compacts using a Siemens D5000 goniometer, 710 X-ray generator using $CuK_\alpha$ radiation at 30 mA, 40 kV. Scans were performed between $2\theta$ values of 5° and 65° with a step size of 0.03° at two seconds per step. Fourier transform infrared (FTIR) spectra were obtained using a Nicolet 800 spectrometer in conjunction with a MTech photo-acoustic (PAS) cell. Spectra were obtained at 4 $cm^{-1}$ resolution averaging 128

[§] *Department of Human Morphology, Medical School, Queens Medical Centre, Nottingham, NG7 2UH.*

0957–4530  

scans. Samples were analysed in the as-received condition and after heat treatment at 1250 °C for 4 h. The calcium to phosphorus ratio and impurity content of the powders were measured by Ceram Research, Stoke-on-Trent using X-ray fluorescence. The morphology of powders was studied with a JEOL 6300 scanning electron microscope with an accelerating voltage of 20 kV. Powder samples were attached to double-sided adhesive carbon tape on a brass stub and sputter coated for approximately one minute using a gold/palladium target. A Micromeritics High Speed Surface Analyser was used to determine particle surface area using the BET method. The volume of nitrogen required to adsorb as a monolayer onto the surface of accurately weighed samples hydroxyapatite was measured at 0 °C and at − 196 °C (liquid nitrogen temperature). The procedure was repeated twice to ensure the reproducibility of the results obtained. Particle size measurements were performed with a Malvern Particle Size Analyser using the 'Mastersizer' software facility. Samples were treated in an ultrasonic bath for one minute using 'Dispex A40' (Allied Colloids Ltd.) in order to break up any loosely bound agglomerates prior to measurement.

## 2.2. Specimen preparation and characterization

Marked differences in the physical characteristics of the powders were found to result in variations in their processing properties. In order to achieve similar densities after sintering at a similar temperature, the specimen preparation conditions had to be carefully controlled. Disc specimens (30 mm diameter by approximately 1.5 mm thickness) were produced using a single action die. A pressure of 14 MPa was exerted using a hydraulic press to produce the discs of powder A. The powder proved to be relatively non-abrasive, was easy to press and resulted in mechanically sound green compacts. Material B proved to be an abrasive powder which produced green compacts which were friable in nature and a maximum pressure of 3 MPa was applied. Samples were then sintered at 1250 °C with heating and cooling rates of 4 °C/min and a dwell of 4 h at the maximum temperature.

## 2.3. Characterization of the sintered specimens

The density of sintered samples was assessed by weighing and measuring. The dimensions of the samples were measured with a micrometer and the mass of the samples was assessed using a five-figure balance. The density of the samples was then calculated and the average taken for the five specimens. The surfaces of the as-sintered ceramics were observed using a JEOL 6300 JSM scanning electron microscope with an accelerating voltage of 10 kV. The grain sizes of the specimens sintered at 1250 °C were measured by applying a linear intercept method to the scanning electron micrographs.

## 2.4. Cell culture

A suspension of human osteosarcoma (HOS) cells (European Collection of Animal Cell Cultures no. 87070202) was prepared in Dulbecco's Modified Eagle's Medium (DMEM, Gibco BRL, Paisley, UK) with added ascorbate (150 μg/ml, Sigma Chemical Co., Poole, UK), L-glutamine (0.02 M, Gibco BRL, Paisley, UK), HEPES (0.01 M Gibco BRL, Paisley, UK) and non-essential amino acids (Gibco BRL, Paisley, UK); the cell density was $0.5 \times 10^4$ cells/ml. The materials were seeded with 1 ml of the cell suspension and incubated (37 °C, 5% $CO_2$) for 15 days. The media was changed every 5 days.

## 2.5. Scanning electron microscopy

The ceramic discs coated with the cells were removed from culture on day 15 and washed twice with Earle's balanced salt solution (Gibco BRL, Paisley, UK) at 37 °C and fixed in 1.5% glutaraldehyde in 0.1 M sodium cacodylate buffer (pH 7.4) overnight. Samples were then dehydrated through a graded methanol series (30%, 50%, 70%, 90%, 96%) to absolute ethanol. These were transferred to absolute acetone for critical point drying with $CO_2$ in a Polaron critical point dryer. Dried samples were sputter coated with gold and examined using a JEOL 35C scanning electron microscope (SEM) operating at 15 kV. Control samples were also prepared in their as-sintered condition and after soaking in culture medium in the absence of cells for 15 days and were observed using a JEOL 6300 microscope with an accelerating voltage of 10 kV.

## 2.6. Transmission electron microscopy

Samples for transmission electron microscopy (TEM) were washed in 0.1 molar sodium cacodylate buffer for 10 min, post-fixed in 1% osmium tetroxide in 0.1 M sodium cacodylate for 30 min, washed in 0.1 M sodium cacodylate buffer twice for 5 min, followed by dehydration twice through a graded series of ethyl alcohol (70%, 80%, 90%, 100%) for 5 min, 30 min in 100% ethyl alcohol (dried with anhydrous sodium sulphate), infiltrated with 1:1 Spurrs' resin/ethyl alcohol for 2 h, followed by two changes of pure resin, embedded and cured for 18 h at 70 °C. After polymerization 0.5–1.0 mm sections were cut from the ceramic discs where the cells appeared to be of the highest density using an annular diamond wheel cutter. These sections were washed briefly in propylene oxide and re-embedded in Spurrs' resin. Sections for TEM were cut on a LKB Ultratome III, picked up onto copper grids with a formvar support, double stained with 2% alcoholic uranyl (10 min) acetate and Reynold's lead citrate (10 min). Sections for X-ray microanalysis were left unstained. A Philips CM12 electron microscope with PV9800 X-ray microanalysis was used at 100 kV for viewing the sections and areas of interest were probed with a spot size between 7 and 15 nm.

### 2.7. Cell turnover and alkaline phosphate production

On day 15 the ceramics were removed from the culture dish and placed into separate dishes. To each dish 1 ml of sterile distilled water was added, the cells then underwent three cycles of freezing at $-70\,^{\circ}C$ for 20 min followed by thawing at $37\,^{\circ}C$ for 15 min to lyse the cells. The cell lysate was then retained for the measurement of DNA and alkaline phosphatase. The alkaline phosphatase activity was measured using the substrate p-nitrophenol phosphate in 1 M diethanolamine buffer pH 9.8 (Diagnostica Merck) using a COBAS BIO centrifugal analyser. For the DNA, 100 μl of cell lysate was digested using 100 μl of papain (Sigma, 1 μl/1 ml of buffer) digest mixture into eppendorfs and incubated at $60\,^{\circ}C$ overnight. The DNA content was then measured on a Perkin-Elmer LS2B fluorimeter at 460 nm.

## 3. Results

### 3.1. Powder characterization

The X-ray diffraction traces for the materials in their as-received condition indicated that the materials were highly crystalline and exhibited no extraneous phases. However, after heat treatment, while powder A remained phase pure, powder B appeared to contain traces ($< 5\%$) of β-TCP.

Infrared spectroscopy results both for the as-received powders and after sintering showed that the materials contained traces of carbonate. There was a broad band shouldered on the OH peak and no disruption in the phosphate bands indicating that the material was hydroxylated. However, the OH peaks in powder B were of a higher intensity than those of powder A. After heat treatment, the carbonate peaks and the O–H peaks at $3600\,cm^{-1}$ in both materials decreased slightly in intensity. Figs 1 and 2 show the infrared traces for materials A and B after heat treatment at $1250\,^{\circ}C$.

The calcium to phosphorus ratios found for the powders are shown in Table I and indicate that while the value for powder B was close to the stoichiometric value for hydroxyapatite (1.67) but calcium deficient, powder A was calcium rich. The levels of trace elements found in the powders with XRF are also shown in Table I. Both powders were found to have similar overall concentrations of impurities, but powder A had higher silica and alumina contents than powder B.

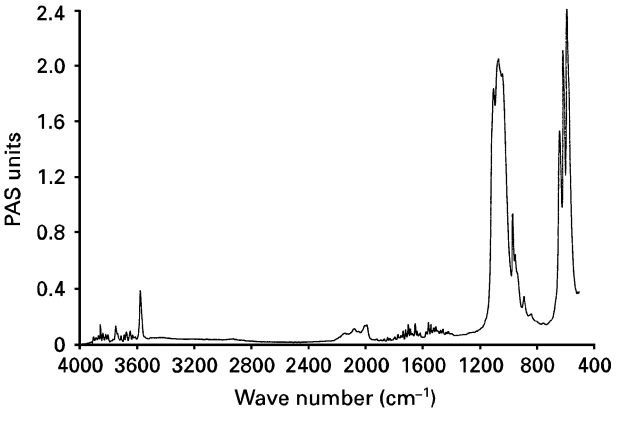


*Figure 1* Infrared trace for powder A after heat treatment at $1250\,^{\circ}C$.

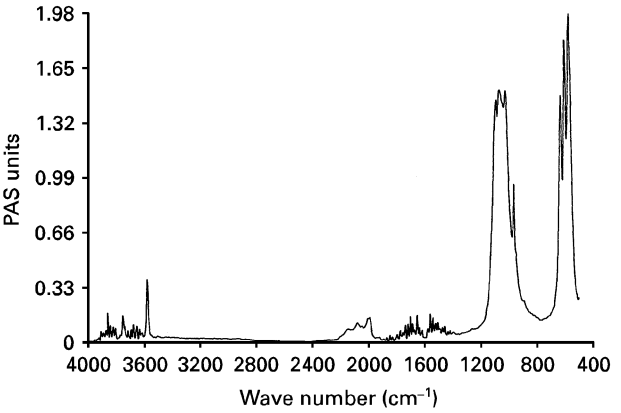


*Figure 2* Infrared trace for powder B after heat treatment at $1250\,^{\circ}C$.

TABLE I X-ray fluorescence results

| Constituent (weight %) | | Powder A | Powder B |
|---|---|---|---|
| Silica | $SiO_2$ | 0.60 | 0.07 |
| Titania | $TiO_2$ | – | 0.01 |
| Alumina | $Al_2O_3$ | 0.10 | 0.03 |
| Ferric oxide | $Fe_2O_3$ | 0.08 | 0.05 |
| Lime | CaO | 54.9 | 54.3 |
| Magnesia | MgO | 0.31 | 0.42 |
| Soda | $Na_2O$ | 0.03 | 0.18 |
| Phosphorus pentoxide | $P_2O_5$ | 39.5 | 41.6 |
| Manganese oxide | $Mn_3O_4$ | 0.01 | 0.01 |
| Strontia | $SrO_2$ | – | 0.02 |
| Calcium to phosphorus ratio | Ca/P | 1.76 | 1.65 |

TABLE II Particle size and surface area analysis results

| Sample | $D_{0.5}$ (μm) | $D_{0.1}$ (μm) | $D_{0.9}$ (μm) | Surface area ($m^2\,g^{-1}$) |
|---|---|---|---|---|
| Powder A | 3.6 | 2.1 | 7.8 | 18 |
| Powder B | 6.0 | 2.5 | 32.5 | 63 |

The surface area and particle size results for the powders are displayed in Table II. The results indicate that the surface area of powder B was more than three times higher than that of powder A. Powder A was found to have a monomodal particle size distribution while that of powder B appeared to be bimodal. The values of the median particle size and the sizes below which 90% and 10% of the particles lie ($D_{0.5}$, $D_{0.9}$ and $D_{0.1}$, respectively) are shown in Table II. The values of $D_{0.1}$, $D_{0.5}$ and $D_{0.9}$ for powder A are all lower than those of powder B.

Scanning electron microscopy of the two powders indicated that powder A appeared to be composed of hard agglomerates of acicular crystallites and that powder B consisted of larger, angular porous agglomerates of spheroid particles approximately 0.5 μm in diameter.

### 3.2. Characterization of the sintered specimens

The densities of the two materials after sintering at 1250 °C are shown in Table III, taking the theoretical density for hydroxyapatite to be 3.156 g $cm^{-3}$. Fig. 3a and b show the surfaces of the sintered materials and indicate that the samples had been pressed and sintered to produce similar grain sizes and densities when sintered to 1250 °C. Intergranular, surface porosity was more evident in material B than in material A, but the surfaces of both materials showed mixed areas of high density and regions of higher porosity. The mean grain size of material B was found be slightly higher than than for material A, but was retained at approximately 2 μm indicating that no accelerated grain growth had taken place.

TABLE III Green and fired densities and grain sizes after sinter ing at 1250 °C

| Specimen | Approx. green density (%) | Density ($g/cm^3$) | Fired density (%) | Grain size (μm) |
|---|---|---|---|---|
| Powder A | 50 | 2.665 | 84.4 | 1.18 |
| Powder B | 40 | 2.675 | 84.7 | 1.89 |

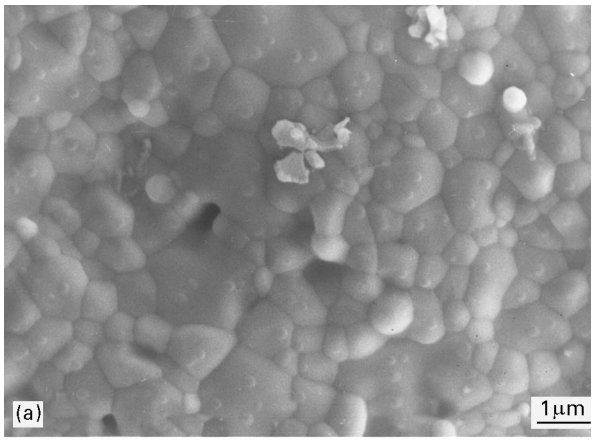


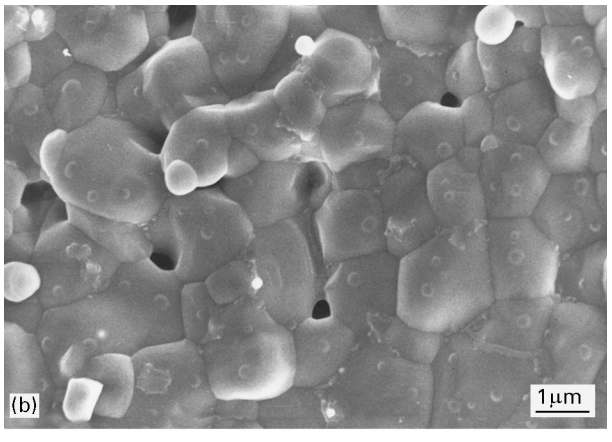


*Figure 3* Scanning electron micrograph of the as-sintered surface of (a) material A, (b) material B.

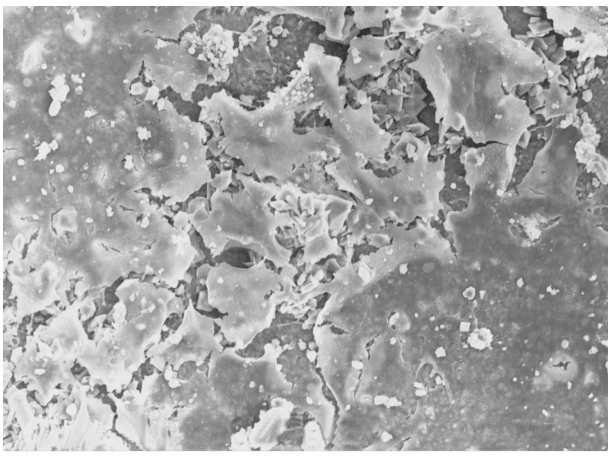

*Figure 4* SEM of osteoblastic cells grown on material A, sintered at 1250 °C. Note that the cells appear in layers and as single cells that are well spread on the surface of the ceramic.

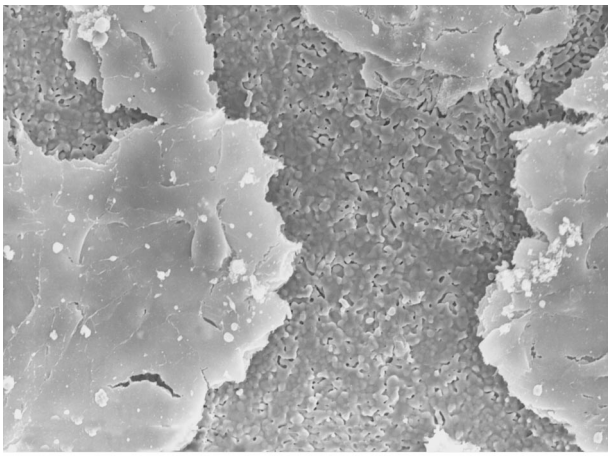

*Figure 5* SEM of osteoblastic cells grown on material B, sintered at 1250 °C. Note that the cells appear as clusters.

### 3.3. Scanning electron microscopy of the cells

The cells were almost 80% confluent with areas of cells that had formed layers. In the areas where single cells could be observed on the surface, the cells appeared to be more spread on material A (Fig. 4). The cells appeared more clustered on material B, with fewer single cells adherent to the surface (Fig. 5). Scanning electron micrographs of the two materials which had been soaked for 15 days in culture medium without being seeded with cells are shown in Fig. 6a and b and revealed that both materials contained areas where little degredation had occurred interspersed with areas of disruption in the grain structure. However, the degree and depth of the disruption in these areas appeared to be more significant for material B than for material A.

### 3.4. Transmission electron microscopy

The transmission electron micrographs of cells grown on material A and material B showed marked differences. The cells on material A appeared normal and

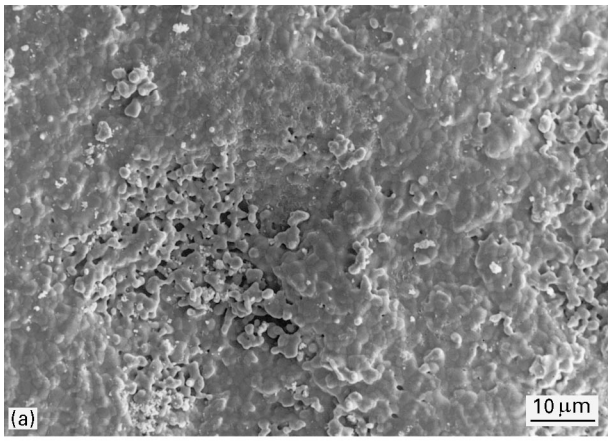


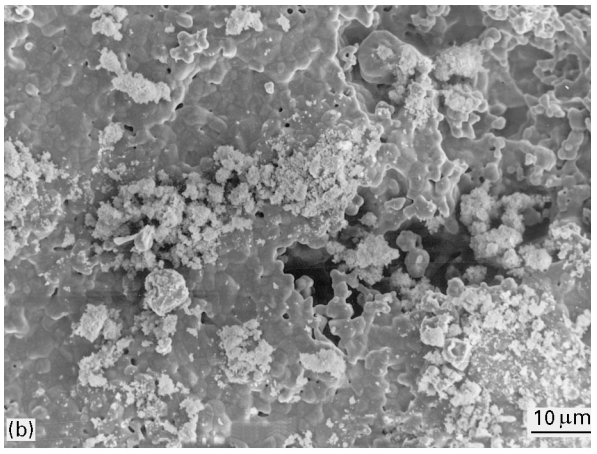


*Figure 6* Scanning electron micrographs after soaking in culture medium for 15 days: (a) material A; (b) material B.

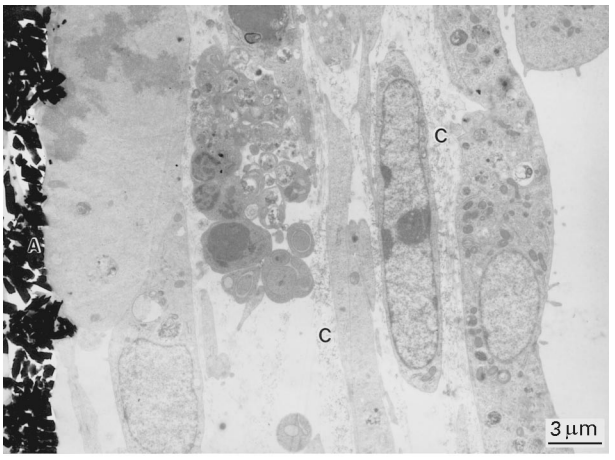


*Figure 7* TEM of osteoblastic cells grown on material A, sintered at 1250 °C. In some areas the cells appeared in layers with a collagenous matrix between the cells. C = collagen, A = material A.

viable. In some areas there were layers of 4–6 cell thickness with a collagenous matrix between the cells (Fig. 7). The ceramics appeared to remain substantially intact, in culture. At higher magnification it could be seen that the cells followed the hydroxyapatite surface and there was no evidence of an interfacial reaction (Fig. 8). The cells on material B appeared less

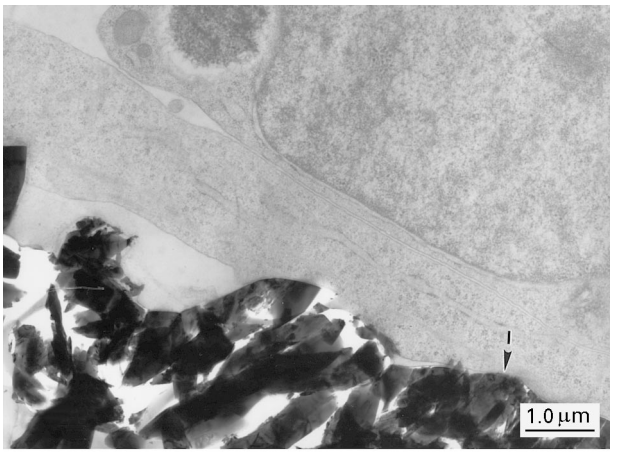


*Figure 8* TEM of osteoblastic cells at the interface of material A. I = interface.

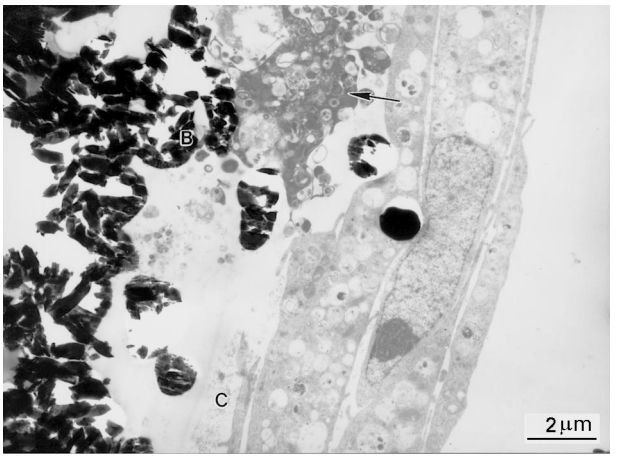


*Figure 9* TEM of osteoblastic cells grown on material B. There was evidence of ceramic degradation and cell death at the interface (arrow). C = collagen, B = material B.

healthy than on material A. There was some evidence of degradation of material B and hydroxyapatite particles were observed within cells at the sample/cell interface (Fig. 9). At higher magnification it could be seen that the cells followed the ceramic surface and there was some evidence of an interfacial reaction (Fig. 10). This was considered to be a biological reaction as the collagen bonding could be observed. X-ray microanalysis of the interfaces with material and the cells showed that no silicon had leached from either of the ceramics nor was there any evidence of a sulphate-rich layer at the interface. The EDAX of material A gave a Ca : P ratio of 1.76 (Fig. 11) while the EDAX of material B gave a Ca : P ratio of 1.65 (Fig. 12).

### 3.5. Cell turnover and alkaline phosphate production

There was almost twice as much AP and DNA in the cells cultured on material A as compared with material B (Table IV). The results clearly show that the rate of cell proliferation but not the rate of alkaline phosphatase production, was highly dependent on the

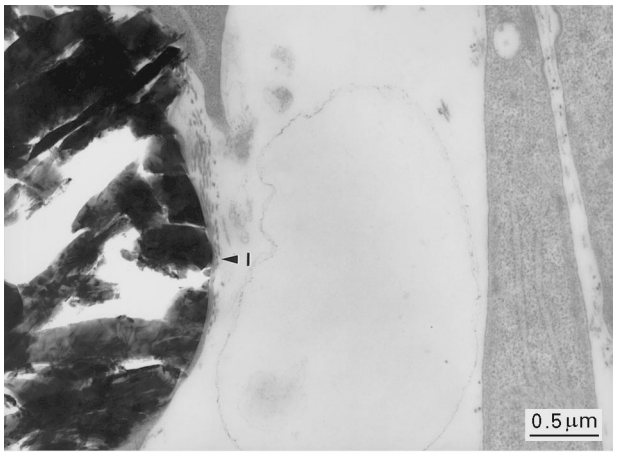


*Figure 10* TEM of osteoblastic cells at the interface of ceramic B. I = interface.

composition of the hydroxyapatite powders that were used to make the ceramic discs.

## 4. Discussion

A number of groups have investigated the use of hydroxyapatite as a bone replacement material [1–10], but it is becoming increasingly obvious that there is significant variability in the physical and chemical characteristics of the material both between batches and from supplier to supplier. This investigation has studied cell response to two materials, which by X-ray diffraction have been shown to have a phase–pure hydroxyapatite structure in their as-received condition. Infrared spectroscopy results both for the as-received powders and after sintering showed that the materials contained traces of carbonate but showed a broad band shouldered on the OH peak and no disruption in the phosphate bands indicating that the material was hydroxylated. However, analysis using X-ray fluorescence revealed that the calcium to phosphorus ratios for the materials deviated significantly from the stoichiometric value for hydroxyapatite: powder A was calcium rich and powder B slightly calcium deficient and the X-ray microanalysis of the ceramics in culture confirmed that there had been no change in the Ca : P ratios. XRF also revealed marked variations in the trace impurity content of the materials and indicated that while powder B was relatively rich in sodium, powder A contained higher levels of silica and alumina. However, it was the difference in calcium to phosphorus ratios between the two materials which resulted in the formation of the β-TCP phase in material B after sintering and probably led to the structural instability observed during cell culture.

Although material B has powder characteristics which would appear to make it more 'active' during sintering, these same powder characteristics resulted in a very friable green compact and due to the pressure applied the green compact density was lower in powder B than in powder A. On sintering, despite the higher driving force for densification, the shrinkage required in powder B to achieve a given density increase was significantly higher than in powder A. Thus, despite the high surface area and bimodal particle size distribution, after sintering for 4 h at 1250 °C, both powders had similar densities and grain sizes although close inspection of the scanning electron micrographs indicated that samples of material B had slightly more surface porosity than samples of material A.

TABLE IV DNA and alkaline phosphatase content of osteoblastic cells on discs after 15 days in culture

| Surface | AP (U/L) | DNA ($mg\,ml^{-1}$) | AP/DNA |
|---|---|---|---|
| Material A | $7.1 \pm 0.50$ | $9.43 \pm 0.51$ | 0.76 |
| Material B | $3.7 \pm 0.80$ | $4.66 \pm 0.68$ | 0.79 |

On subsequent *in vitro* testing, the performance of material B appeared to be inferior to material A in the following ways: the cells appeared to be more spread on material A and more clustered on material B, with fewer single cells adherent to the surface; the cells on material A appeared normal and viable with no evidence of an interfacial reaction, whereas for material B the cells appeared to be less healthy; there was some evidence of degradation of material B and ceramic particles were observed within cells at the ceramic interface with some evidence of an interfacial reaction; there was almost twice as much AP and DNA in the cells cultured on ceramic A as compared with ceramic B.

The differences in cell behaviour appear to have been due to one, or a combination, of the factors below:

(a) the difference in the calcium to phosphorus ratio of the materials leading to:
(b) the formation of trace amounts of TCP in material B;
(c) differences in the trace impurity content between the two powders;
(d) slightly higher surface porosity in material B.

It is probable that the cellular response observed for material B was due to a combination of these factors. The inferior mechanical and *in vivo* stability of tricalcium phosphate have been reported in the past [5, 27]. While in some cases the resorption of a ceramic implant may be desirable, in this study the degredation of material B was associated with a poorer cellular response. The degredation could have been due to inferior mechanical performance or higher solubility, but in either case, the subsequent increase in surface area may have resulted in an increase in the amount of impurity ions released.

The behaviour of calcium phosphates in cell culture have been reported previously [17–20] but the cell types have been animal in origin and characterization of the substrate material has been concentrated on only one of the parameters listed above. This paper indicates the importance of full characterization of

two nominally similar materials in order that differences in cell response to hydroxyapatite reported in the literature may be more fully understood.

## 5. Conclusion

The work reported in this paper indicates the great importance of full characterization of the materials being used. Both materials were supplied as high purity hydroxyapatites and characterization revealed that in their as-received condition both materials were crystallographically phase–pure hydroxyapatite. However, they exhibited markedly different calcium to phosphorus ratios, trace element impurities, ceramic handling properties and sintering characteristics and these differences led to a strong variation in cellular response to each material.


## Acknowledgements

The authors gratefully acknowledge the funding of this work by the Engineering and Physical Sciences Research Council. We would also like to thank Dr Jonathan Knowles, Dr Ray Smith and Dr Ihtesham Rehman of the IRC in Biomedical Materials, Queen Mary and Westfield College, for their help with the X-ray diffraction and FTIR work.


## References


1. M. AKAO, H. AOKI and K. KATO, *J. Mater. Sci.* **16** (1981) 809.
2. H. W. DENISSEN, K. DEGROOT, A. A. DRIESSEN, J. G. C. WOLKE, J. G. J. PEELEN, H. J. A. VAN DIJK, A. P. GEHRING and P. J. KLOPPER, *Sci. Ceram.* **10** (1980) 63.
3. G. DE WITH, H. J. A. van DIJK and N. HATTU, *Proc. Brit. Ceram. Soc.* **31** (1981) 181.
4. G. DE WITH, H. J. A. van DIJK, N. HATTU and K. PRIJS, *J. Mater. Sci.* **16** (1981) 1592.
5. A. A. DRIESSENS, C. P. A. T. KLEIN and K. DEGROOT, *Biomaterials* (*Commun.*) **3** (1982) 113.
6. M. JARCHO, C. H. BOLEN, M. B. THOMAS, J. BOBICK, J. F. KAY and R. H. DOREMUS, *J. Mater. Sci.* **11** (1976) 2027.
7. T. KIJIMA and M. TSUTSUMI, *J. Amer. Ceram. Soc.* **62** (1979) 455.
8. H. ROOTARE and R. G. CRAIG, *J. Oral Rehab.* **5** (1978) 293.
9. M. B. THOMAS, R. H. DOREMUS, M. JARCHO and R. L. SALSBURY, *J. Mater. Sci.* **15** (1980) 891.
10. H. NAGAI and Y. NISHIMURA, US Patent no. 4,548,59, October 1985.
11. S. BEST, W. BONFIELD and C. DOYLE, in Bioceramics 1: Proceedings of the 1st International Bioceramic Symposium, edited by H. Oonishi, H. Aoki and K. Sawai (Ishiyaku Euro-America Inc., 1989) pp. 68–73.
12. *Idem.*, in Bioceramics 2: Proceedings of the 2nd International Symposium on Ceramics in Medicine, edited by G. Heimke (Deutsche Keramische Gesellschaft e.V, 1990) pp. 57–64.
13. S. PUAJINDANETR, S. BEST and W. BONFIELD, in Bioceramics 5: Proceedings of the 5th International Symposium on Ceramics in Medicine, edited by T. Yamamuro, T. Kukubo and T. Nakamura (Kobunshi Kankikai Inc., 1992) pp. 23–29.
14. *Idem. Brit. Ceram. Trans.* **93** (1994) 96.
15. S. BEST and W. BONFIELD, *J. Mater. Sci. Mater. Med.* **5** (1994) 516.
16. S. BEST, PhD thesis, University of London, 1990.
17. B. T. GARVEY and R. BIZIOS, *J. Appl. Biomater.* **5** (1984) 39.
18. M. AKAO, M. SAKATSUME, H. AOKI, T. TAKAGI and T. S. SASAKI, *J. Mater. Sci. Mater. Med.* **4** (1993) 569.
19. F. B. BAGAMBISA, U. JOOS and W. SCHILLI, *Int. J. Oral Maxillofacial Implants* **5** (1990) 217.
20. D. A. PULEO, L. A. HOLLERAN, R. H. DOREMUS and R. BIZIOS, *J. Biomed. Mater. Res.* **25** (1991) 711.
21. M. F. BASLE, A. REBEL, F. GRIZON, G. DACULSI, N. PASSUTI and R. FILMAN, *J. Mater. Sci. Mater. Med.* **4** (1993) 273.
22. R. G. T. GEESINK, K. DE GROOT and C. P. A. T. KLEIN, *J. Bone Joint Surg.* **70-B** (1988) 17.
23. J. A. JANSEN, J. P. C. M. VAN DER WAERDEN and J. G. C. WOLKE, *J. Mater. Sci. Mater. Med.* **4** (1993) 466.
24. C. P. A. T. KLEIN, P. PATKA, J. G. C. WOLKE, J. M. A. de BLIECK-HOGERVORST and K. de GROOT, *Biomaterials* **15** (1994) 146.
25. A. WILKE, J. ORTH, M. KRAFT and P. GRISS, *J. Mater. Sci. Mater. Med.* **4** (1993) 260.
26. K. SØBALLE, E. S. HANSEN, H. BORKSTEDT-RASMUSSEN, P. H. JØRGENSEN and C. BÜNGER, *J. Orthop. Res.* **10** (1992) 285.
27. R. Z. LEGEROS, *Adv. Dent. Res.* **2** (1988) 164.



*Received 10 January*
*and accepted 3 March 1996*